Electro-optical properties of Cu_2O for P excitons in the regime of Franz-Keldysh oscillations

Sylwia Zielińska-Raczyńska, David Ziemkiewicz,* and Gerard Czajkowski
Institute of Mathematics and Physics, UTP University of Science and Technology, Aleja Prof. S. Kaliskiego 7, 85-789 Bydgoszcz, Poland

(Received 16 December 2017; revised manuscript received 14 March 2018; published 19 April 2018)

We present the analytical method which enables one to compute the optical functions i.e., reflectivity, transmission, and absorption, including the excitonic effects, for a semiconductor crystal exposed to a uniform electric field for the energy region above the gap and for the external field suitable for the appearance of Franz-Keldysh (FK) oscillations. Our approach intrinsically takes into account the coherence between the carriers and the electromagnetic field. We quantitatively describe the amplitudes and periodicity of FK modulations as well as the influence of Rydberg excitons on the FK effect. Our analytical findings are illustrated numerically for P excitons in Cu_2O crystal.

DOI: 10.1103/PhysRevB.97.165205

I. INTRODUCTION

A lot of studies, both experimental and theoretical, have been devoted to examining various properties of excitons in Cu_2O bulk crystal, and it appeared that the spectroscopical features of copper oxide were recognized throughout (see Refs. [1–7]). But recently, the interest in this bulk semiconductor has reignited due to an outstanding experiment performed by Kazimierczuk *et al.* [8], who discovered highly excited states, so-called Rydberg excitons (RE), in the natural crystal of copper oxide. They have observed absorption lines associated with excitons of principal quantum numbers up to $n = 25$.

A large number of new studies focused on the extraordinary properties of RE have attracted increasing attention during the last three years [9–17], especially regarding their behavior in external fields [18–20] as well as in the context of the similarity of their spectra to quantum chaos and breaking all antiunitary symmetries [21–23]. Recently, an observation of photoluminescence of excitonic Rydberg states was reported [24].

Until now, much effort has been devoted to examining excitons in Cu_2O for energies below the gap, the region in which the most important effect, i.e., the appearance of excitons with a high number n, has been observed. One distinct peculiarity of copper oxide is the moderately small Rydberg energy of only 90 meV, which ensures that all relevant states from the ground state up to the continuum above the band gap are optically accessible using attainable lasers.

Recently, some attempts [25] have been reported in which the optical properties of Cu_2O for excitation energies exceeding the fundamental gap were examined. Heckötter *et al.* [25], using two-color pump-probe spectroscopy, studied RE in copper oxide in the presence of free carriers injected by above-band-gap excitation. They examined the impact of an ultralow-density plasma on Rydberg excitations at the temperature of a few kelvins and observed that inside a Cu_2O crystal plasma shifts the band edge downwards, diminishing the maximum excitable Rydberg state, which, in turn, leads to modulation of the plasma blockade induced by the band gap modulation.

Below we study another effect that appears for above-gap excitation, electro-optic properties. For excitation energies below the gap, the main electro-optic effects are the shifting, splitting, and, for higher excitonic states, mixing of spectral lines [18]. Like for direct-band semiconductors, for energies above the gap and when a constant electric field is applied, specific oscillations in the spectra, known as the Franz-Keldysh oscillations, have been observed [26–41].

These oscillations are results of wave functions "leaking" into the band gap; the key mechanism of this effect is photon-assisted tunneling across the band gap. When an electric field is applied, the electron and hole wave functions become Airy functions rather than plane waves (and they have a "tail" which extends into the classically forbidden band gap). Due to the influence of the electric field on interband transitions in the presence of excitons the dielectric constant of a semiconductor exhibits Franz-Keldysh oscillations, which can be detected by modulated reflectance. The Franz-Keldysh (FK) effect, which gives the possibility of creating and controlling reflectivity oscillations, provides a key ingredient to the goal of achieving a precise tool for steering on-demand periodicity and amplitude of electromodulations. The FK effect has also had practical applications (see, for example, Ref. [42]).

The theoretical description of the FK effect is quite different from that for all the phenomena below the gap. For energies below the gap a well-known solution of a hydrogenlike Schrödinger equation can be used in which the term related to the applied electric field is treated as a perturbation [18]. For energies above the gap one deals with the continuum states. When the electric field is applied, the relevant material (constitutive) equation contains terms of different symmetries, so an analytical solution is not known.

As mentioned by Ralph [30], to the best of our knowledge the FK effect has not been examined experimentally for the Cu_2O bulk crystal.

Here we develop the real density-matrix approach previously used to describe optical properties of Rydberg excitons below the gap [10,18,20], including energies above the gap

*david.ziemkiewicz@utp.edu.pl

and taking into account the changes caused by an externally applied electric field, whose intensity should be small enough to avoid Stark localization but sufficient to enable observation of Franz-Keldysh oscillations. The Franz-Keldysh effect gives the possibility to create and control reflectivity oscillations. Circumventing this problem would be a key to achieve the goal of precisely steering on-demand periodicity and amplitude of electromodulations. Below we show that using excitons, one gets a flexible tool to study the oscillation dynamics of reflectivity of a Cu_2O crystal irradiated by electromagnetic radiation and affected by an electric field. The tunability, which can be exploited to force the desired period and amplitude of modulations, can be achieved through the modification of an external electric field intensity, which in turn influences the excitonic levels' shifting and overlapping. Moreover, the periodic FK oscillations can be used to determine the effective masses along the axes of propagation inside the crystal.

This paper is organized as follows. In Sec. II we sketch the outline and present general density-matrix equations governing the evolution of the system, which are necessary to calculate the macroscopic polarization of a medium. These general considerations are then specified for the case of Cu_2O in Secs. III and IV, where we show the appearance of the Franz-Keldysh effect. Section V contains a discussion of how more excitonic states can be accounted for in the calculations of the FK effect with illustrative examples of susceptibility for Cu_2O. In Sec. VI the general approach in which each of the excitonic states is described by appropriate harmonic oscillators is presented. Such a procedure allows one to calculate the electrosusceptibility for any energetic region (below and above the gap). The particular case of a P exciton for energies above the gap is also discussed in this section. The conclusions are discussed in Sec. VII.

II. DENSITY-MATRIX FORMULATION

We intend to calculate the optical functions of a Cu_2O crystal when a homogeneous electric field is applied in the z direction, which is chosen to be perpendicular to the crystal surface, and the excitation energy exceeds the fundamental gap energy. The method is based on the so-called real density-matrix approach (RDMA) which, for a similar physical situation but with excitation energy below the gap, was used in Ref. [18]. The kernel of the RDMA is the so-called constitutive equation

$$\dot{Y}(\mathbf{R},\mathbf{r}) + (i/\hbar)H_{eh}Y(\mathbf{R},\mathbf{r}) + (1/\hbar)\Gamma Y(\mathbf{R},\mathbf{r}) = (i/\hbar)\mathbf{M}(\mathbf{r})\mathbf{E}(\mathbf{R}), \tag{1}$$

where Y is the bilocal coherent electron-hole amplitude (pair wave functions), $\mathbf{R}$ is the excitonic center-of-mass coordinate, $\mathbf{r} = \mathbf{r}_e - \mathbf{r}_h$ is the relative coordinate, $\mathbf{M}(\mathbf{r})$ is the smeared-out transition dipole density, and $\mathbf{E}(\mathbf{R})$ is the electric field vector of the wave propagating in the crystal. The coefficient Γ in the constitutive equation represents dissipative processes. The two-band effective mass Hamiltonian H_{eh} of the system under a constant electric field $\mathbf{F} = (0,0,F)$ that includes the electron and hole kinetic energy terms, the electron-hole interaction potential, and the confinement potentials [10] has the form

$$H_{eh} = E_g - \frac{\hbar^2}{2m_e}\partial_{z_e}^2 - \frac{\hbar^2}{2m_h}\partial_{z_h}^2 - \frac{\hbar^2}{2\mu}\left(\partial_x^2 + \partial_y^2\right) - \frac{\hbar^2}{2M_{\text{tot}}}\left(\partial_{R_\parallel}^2 + R_\parallel^{-1}\partial_{R_\parallel}\right) + eF(z_h - z_e) + V_{eh}(z_e - z_h,\rho) + V_e(z_e) + V_h(z_h), \tag{2}$$

where we have separated the center-of-mass coordinate $R_\parallel$ from the relative coordinate ρ on the plane x-y. The potential term representing the Coulomb interaction in an anisotropic medium is given by

$$V_{eh} = -\frac{e^2}{4\pi\epsilon_0\epsilon_b[(x^2+y^2)+z^2]^{1/2}}, \tag{3}$$

with ϵ_b being the bulk dielectric constant. The smeared-out transition dipole density $\mathbf{M}(\mathbf{r})$, which should be chosen in our case to be appropriate for P or F excitons [20], is related to the bilocality of the amplitude Y and describes the quantum coherence between the macroscopic electromagnetic field and the interband transitions.

The coherent amplitude Y defines the excitonic counterpart of the polarization

$$\mathbf{P}(\mathbf{R}) = 2\int d^3r \,\text{Re}[\mathbf{M}(\mathbf{r})Y(\mathbf{R},\mathbf{r})], \tag{4}$$

which is then used in the Maxwell propagation equation

$$c^2\nabla_R^2\mathbf{E} - \underline{\underline{\epsilon}}_b\ddot{\mathbf{E}}(\mathbf{R}) = \frac{1}{\epsilon_0}\ddot{\mathbf{P}}(\mathbf{R}), \tag{5}$$

where $\underline{\underline{\epsilon}}_b$ is the bulk dielectric tensor and ϵ_0 is the vacuum dielectric constant. In the present paper we solve Eqs. (1)–(5) in order to compute the electro-optical functions (i.e., reflectivity, transmission, and absorption) for Cu_2O. Contrary to the previous paper on electro-optical properties [18], we will consider the excitation energies above the energy gap, which will require a more general approach.

Both polarization and electric field must obey Maxwell's equations, which have to be solved in order to get the propagation modes. The above approach takes into account key factors necessary for the calculation of all optical functions. They are obtained, as usual, by comparing the amplitudes of incident, reflected, or transmitted electric fields and depend on the applied field strength and on the total crystal thickness.

III. THE BASIC EQUATIONS

The considered crystal is modeled by a slab with infinite extension in the xy plane and the boundary planes $z = 0, z = L$. For the sake of simplicity, the slab is located in vacuum. A monochromatic, linearly polarized electromagnetic wave propagates along the z axis. Its electric field is given by

$$\mathbf{E} = (0,E_y,0), \quad E_y = E_{\text{in}}e^{ik_0z - i\omega t}, \tag{6}$$

where $k_0 = \omega/c$ is the wave vector in the vacuum, with ω being the frequency, and E_{in} is the amplitude of the incoming wave. Due to the fact that the energy of the propagating wave is divided into reflected and transmitted waves one obtains the

reflectivity and transmissivity from the following relations:

$$R = \left|\frac{E(0)}{E_{\text{in}}} - 1\right|^2, \quad T = \left|\frac{E(z=L)}{E_{\text{in}}}\right|^2, \tag{7}$$

where $E(z)$ is the y component of the wave's electric field inside the crystal. We will calculate the optical functions for the case when a constant electric field F is applied in the z direction. The calculation of the optical functions consists of several steps. The first one is the solution of the constitutive equation (1). Due to the specific properties of Cu_2O, we will treat the crystal as the bulk region and assume the amplitude Y and the wave electric field E have the forms

$$Y(Z,\mathbf{r}) = Y(\mathbf{r})e^{ik_z Z}, \quad \mathbf{E}(Z) = \mathbf{E}_0 e^{ik_z Z}. \tag{8}$$

Assuming the wave propagation is in the z direction and accounting for the properties of Cu_2O, we neglect the $R_\parallel$ component and the confinement potentials, arriving at the equation

$$\left[E_g - \hbar\omega - i\Gamma + \frac{\hbar^2 k_z^2}{2M_{\text{tot}}} - \frac{\hbar^2}{2\mu}\partial_z^2 - \frac{\hbar^2}{2\mu}\left(\partial_x^2 + \partial_y^2\right) + eFz + V_{eh}(z,\rho)\right] Y(x,y,z) = \mathbf{M}(\mathbf{r})\mathbf{E}(Z), \tag{9}$$

where M_{tot} and μ are the exciton total and reduced effective masses, respectively. For further considerations we must specify the dipole density $\mathbf{M}$. Due to the symmetry properties of Cu_2O the total symmetry of the excitons' state must be the same as the symmetry of the dipole operator, and according to this, the transition dipole density appropriate for P excitons will be considered. This will result in the shapes of the real and imaginary parts of the electrosusceptibility. In previous papers [18,20], for energies below the gap, we took the dipole density in terms of spherical coordinates. For energies above the gap and with the applied electric field, the cylindrical symmetry must be used. For the sake of simplicity, we use the in-plane components of the dipole density with the coherence radius r_0 along the planes and zero in the growth direction.

The cylindrical version of the formula for the M_y component of the P exciton in Cu_2O, given in Ref. [10], has the form

$$M(\rho,\zeta,\phi) = \frac{1}{2}M_0\sqrt{\frac{2}{\pi}}\frac{\rho}{\rho_0^3}e^{-\rho^2/2\rho_0^2}\frac{e^{i\phi}+e^{-i\phi}}{\sqrt{2\pi}}\delta(\zeta). \tag{10}$$

Here we used the dimensionless quantities

$$\rho = \frac{\sqrt{x^2+y^2}}{a^*}, \quad \zeta = \frac{z}{a^*}, \tag{11}$$

and ρ_0 is the coherence radius. For further discussion we define the quantities

$$f = \frac{F}{F_{\text{I}}}, \quad k^2 = \frac{2\mu}{\hbar^2}a^{*2}(E_g - \hbar\omega - i\Gamma) + \frac{\mu}{M_{\text{tot}}}\left(k_z^2 a^{*2}\right), \tag{12}$$

where F_{I} is the so-called ionization field

$$F_{\text{I}} = \frac{\hbar^2}{2\mu_\parallel e a^{*3}} = \frac{R^*}{a^* e}, \tag{13}$$

with R^* being the excitonic Rydberg and a^* being the corresponding excitonic Bohr radius. We also use the so-called electro-optic energy

$$\hbar\Theta = R^* f^{2/3} = \left(\frac{\hbar^2}{2\mu}\right)^{1/3}(eF)^{2/3}. \tag{14}$$

With these quantities Eq. (9) can be rewritten in the form

$$\left(k^2 - \partial_\rho^2 - \frac{1}{\rho}\partial_\rho - \frac{1}{\rho^2}\partial_\phi^2 - \partial_\zeta^2 + f\zeta\right)Y = \frac{2\mu}{\hbar^2}a^{*2}ME_y + \frac{2}{\sqrt{\rho^2+\zeta^2}}Y. \tag{15}$$

M denotes the relevant component of the dipole density, given by Eq. (10), and E_y is the y component of the electric wave field.

IV. THE ELECTROSUSCEPTIBILITY AND FRANZ-KELDYSH EFFECT FOR THE P EXCITON

In this section we derive the expression for the bulk Cu_2O electrosusceptibility for the P exciton. Following the procedure described in Ref. [36], we separate the Hamiltonian in Eq. (1) transformed to the form in (15) into a kinetic + electric field part $H_{\text{kin+F}}$ and a potential term V which lead to the following form of the basic constitutive equation (1):

$$H_{\text{kin+F}}Y = \mathbf{ME} - VY. \tag{16}$$

The above expression corresponds to THE Lippmann-Schwinger equation, in which the Green's function G appropriate for the kinetic + electric field part is adopted for the coherent amplitude

$$Y = G\mathbf{ME} - GVY. \tag{17}$$

The Green's function for Eq. (15) has the form

$$G(\rho,\rho';\zeta,\zeta';\phi,\phi') = \frac{1}{2\pi}\sum_{m=-\infty}^{\infty} e^{im(\phi-\phi')} \times \int_0^\infty x\,dx\, J_m(x\rho)J_m(x\rho')g_x(\zeta,\zeta'), \tag{18}$$

where

$$g_x(\zeta,\zeta') = g^<\, g^>,$$
$$g^< = \frac{\pi}{f^{\frac{1}{3}}}\left\{\text{Bi}\left[f^{\frac{1}{3}}\left(\zeta^< + \frac{k^2+x^2}{f}\right)\right] + i\,\text{Ai}\left[f^{\frac{1}{3}}\left(\zeta^< + \frac{k^2+x^2}{f}\right)\right]\right\},$$
$$g^> = \text{Ai}\left[f^{\frac{1}{3}}\left(\zeta^> + \frac{k^2+x^2}{f}\right)\right], \tag{19}$$

J_m are Bessel functions, and Ai(z) and Bi(z) are Airy functions (see Ref. [43]). To obtain the optical functions one has to solve Eq. (17) using the Green's function (18). Please note that Eq. (17) has the form of the Fredholm integral equation of the second type. There are many methods of solving such equations [44], and the particular choice depends on the specific properties of the particular crystal. One of the methods uses a certain form of the function Y (ansatz) which depends on an unknown parameter Y_0. The parameter is then obtained from

Eq. (17) and used to calculate the polarization from Eq. (4) and the electric field of the wave from Eq. (5).

The ansatz for Y will be taken in the form

$$Y = Y_0 \rho \frac{e^{i\phi} + e^{-i\phi}}{\sqrt{2\pi}} \exp(-k\sqrt{\rho^2 + \zeta^2}), \tag{20}$$

which has the symmetry of the $2P$ exciton state. With the above ansatz, the Green's function (18), and the M_y dipole density (10), we obtain the following expression for the susceptibility:

$$\begin{aligned}\chi &= 2\frac{|M_0|^2 2\mu}{\epsilon_0 a^* \hbar^2 f^{\frac{1}{3}} Q} \int_0^\infty x^3 dx \exp(-\rho_0^2 x^2)\left[\mathrm{Bi}\left(\frac{k_x^2}{f^{\frac{2}{3}}}\right)\right. \\ &\left. + i\,\mathrm{Ai}\left(\frac{k_x^2}{f^{\frac{2}{3}}}\right)\right]\mathrm{Ai}\left(\frac{k_x^2}{f^{\frac{2}{3}}}\right)\frac{\tilde{M}Y}{M_0 Y_0} \\ &= \frac{2\pi\rho_0^3 \chi'}{Q} f\, e^{-\mathcal{E}\rho_0^2} \int_{-\mathcal{E}}^\infty du\, e^{-\rho_0^2 f^{2/3} u}(u + \mathcal{E})[\mathrm{Bi}(u) \\ &+ i\,\mathrm{Ai}(u)]\mathrm{Ai}(u),\end{aligned} \tag{21}$$

with

$$\chi' = \frac{2}{\epsilon_0}\frac{2\mu}{\hbar^2 a^*}\frac{M_0^2}{4\pi\rho_0} \tag{22}$$

and

$$\begin{aligned} k_x^2 &= k^2 + x^2, \\ u &= \frac{k^2 + x^2}{f^{2/3}}, \\ \mathcal{E} &= \frac{\hbar\omega + i\Gamma - E_g}{\hbar\Theta}, \\ \frac{\tilde{M}Y}{M_0 Y_0} &= \sqrt{\frac{2}{\pi}}\rho_0 \Gamma(4) \exp\left(k^2\rho_0^2/4\right) D_{-4}(k\rho_0), \end{aligned}$$

where $\hbar\Theta$ is the electro-optical energy (14) and D_{-4} is the parabolic cylinder function (see, for example, [43,45]),

$$\begin{aligned} D_p(z) &= \frac{\exp(-z^2/4)}{\Gamma(-p)} \int_0^\infty e^{-xz-(x^2/2)} x^{-p-1} dx \\ &(\mathrm{Re}\, p < 0), \end{aligned} \tag{23}$$

with Γ being the Euler gamma function. The expression Q appearing in the denominator in (21) is given by

$$Q = \frac{(\tilde{M}Y) - \tilde{M}G|V|Y}{M_0 Y_0}, \tag{24}$$

where

$$\begin{aligned} MG|V|Y &= M_0 Y_0 \rho_0 \sqrt{\frac{2}{\pi}}\frac{2\pi}{f^{1/3}} \int_0^\infty x^3\, dx e^{-\rho_0^2 x^2/2} \mathrm{Ai}\left(\frac{k_x^2}{f^{2/3}}\right) \\ &\times \int_0^\infty d\zeta \left(\frac{\zeta}{k_x^2} + \frac{1}{k_x^3}\right) e^{-k_x\zeta} \left\{\mathrm{Bi}\left[f^{1/3}\left(\frac{k_x^2}{f} - \zeta\right)\right]\right. \\ &\left. + i\,\mathrm{Ai}(f^{1/3}\left(\frac{k_x^2}{f} - \zeta\right))\right\} + M_0 Y_0 \rho_0 \sqrt{\frac{2}{\pi}}\frac{2\pi}{f^{1/3}} \\ &\times \int_0^\infty x^3\, dx e^{-\frac{\rho_0^2 x^2}{2}} \left[\mathrm{Bi}\left(\frac{k_x^2}{f^{2/3}}\right) + i\,\mathrm{Ai}\left(\frac{k_x^2}{f^{2/3}}\right)\right] \\ &\times \int_0^\infty d\zeta e^{-k_x\zeta}\left(\frac{\zeta}{k_x^2} + \frac{1}{k_x^3}\right)\mathrm{Ai}\left[f^{1/3}\left(\frac{k_x^2}{f} + \zeta\right)\right]. \end{aligned} \tag{25}$$

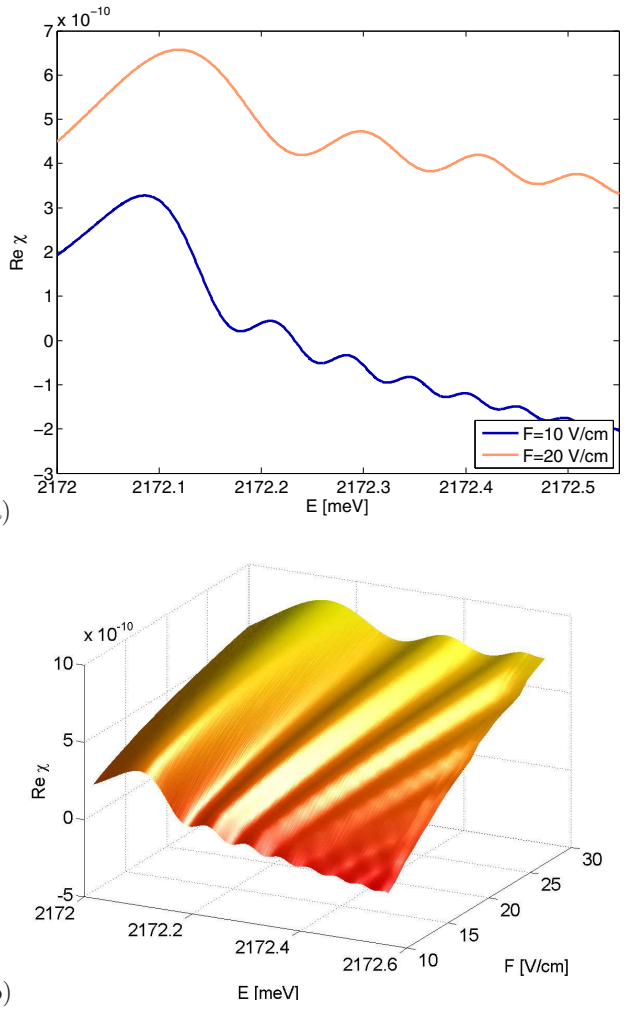

FIG. 1. Real part of the electrosusceptibility for a Cu_2O crystal in the energetic region of Franz-Keldysh oscillations, calculated with formula (21) and taking into account the excitonic effect, (a) for two values of the electric field strength ($F = 10$V/cm and $F = 20$ V/cm) and (b) for a range of values of F. The coherence radius is $\rho_0 = 0.2a^*$, $\Gamma = 0.8$ meV.

The vanishing of the real part of Q gives the resonances of the susceptibility. In particular, for the case without electric field $F = 0$, one obtains

$$\frac{\tilde{M}G|V|Y}{M_0 Y_0} = M_0 Y_0 \rho_0 \sqrt{\frac{2}{\pi}}\frac{1}{2k}\Gamma(4) e^{z^2/4} D_{-4}(k\rho_0). \tag{26}$$

Some unique features of the susceptibility can be read off directly from formula (21). In particular, for energies above the gap (i.e., for $\hbar\omega > E_g$) we obtain the FK oscillations in the spectrum, which appear due to the periodic character of Airy functions Ai and Bi.

Some quantitative properties of the spectrum can be obtained by neglecting the electron-hole interaction, i.e., by taking $V = 0$. The results for the susceptibility from formula (21) with Q calculated from Eq. (24) are shown in Fig. 1 (the real part) and Fig. 2 (the imaginary part) for two values of the applied electric field. The two values are inserted into formula (A10), which gives the corresponding values of χ'.

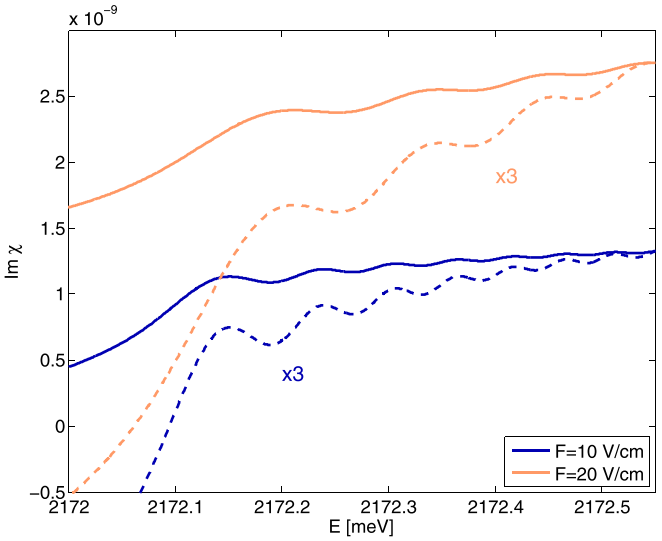

FIG. 2. The same as in Fig. 1(a) for the imaginary part of the susceptibility. For clarity, oscillations are enlarged and marked by dashed lines.

We have used the parameter values appropriate for Cu_2O: $E_g = 2172\,\text{meV}, m_e = 0.985m_0, m_h = 0.575m_0$ [46], with m_0 being the free-electron mass. With those masses one obtains the reduced mass as $\mu = 0.363m_0$. The Rydberg energy and the excitonic Bohr radius are then obtained from

$$R^* = \frac{\mu \times 13\,600\ \text{meV}}{\epsilon_b^2}, \quad a^* = \frac{\epsilon_b}{\mu} a_0. \tag{27}$$

Taking the values $\epsilon_b = 7.5$ and $a_0 = 0.0529$ nm, we obtain $R^* = 87.78$ meV and $a^* = 1.1$ nm. The quantity χ' [see Eq. (A10)], related to the oscillator strength, depends on the $L - T$ energy Δ_{LT} for which we have used the value $1.25\,\mu$eV [47]. We have performed the calculations for two values of damping, $\Gamma = 0.4$ meV and $\Gamma = 0.8$ meV; the latter value of Γ corresponds to that calculated by Stolz *et al.* [47] for the $n = 2$ state of the P exciton in Cu_2O. It can be seen from Figs. 1 and 2 that for excitation energies $E = \hbar\omega$ above the gap noticeable oscillations in the real and imaginary parts of the susceptibility appear. Their period and amplitude increase with field strength.

The effects of coherence between the quantum effects (here the FK oscillations) and the macroscopic incoming wave are incorporated into the shape of the transition dipole density $M(\mathbf{r})$, characterized by the matrix element M_0 and the coherence radius ρ_0. In the presented model the two parameters are not independent, and the relation between them is discussed in Appendix A. Here we used ρ_0 as a free parameter, which was also done in previous papers in which the real density-matrix approach was used [10,18]. The dependence of the susceptibility on the coherence radius and energy is shown in Fig. 3. In the subsequent plots, we have taken $\rho_0 = 0.2a^*$ [10].

For the purpose of illustration we show in Figs. 4 and 5 the real and imaginary parts of the derivative $\partial\chi/\partial E$, for which the FK oscillations are more evident. It should be noted that the external field should be chosen carefully, i.e., be small enough to avoid Stark localization but sufficiently strong for oscillation to manifest.

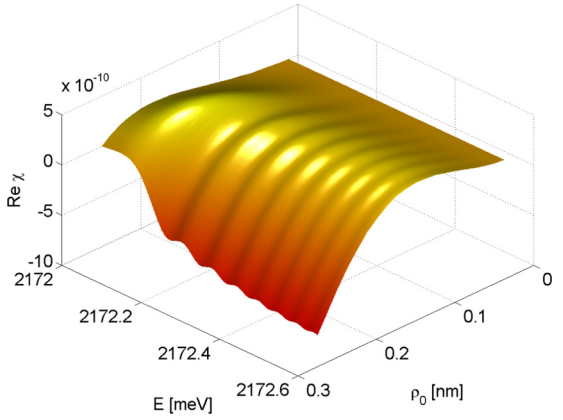

FIG. 3. The same as in Fig. 1(b) at fixed value of the electric field, $F = 10\,\text{V/cm}$, for a range of values of ρ_0.

It can be proved (see Ref. [48] and Appendix B) that the peaks of FK oscillations observed in Figs. 1–5 appear at energies

$$(E_n - E_g)^{3/2} = \frac{3}{4} n\pi (\hbar\theta)^{3/2} = \frac{3n\pi e\hbar F}{4\sqrt{2\mu}}. \tag{28}$$

The above formula contains all extrema. It follows from Eq. (B4) that for $\Gamma \to 0$ FK oscillations appear around a curve $(\hbar\omega - E_g)^{3/2}$. The slope is analogous to that obtained for forbidden transitions [28,29,40] and differs from that observed for S excitons, which in turn depends on $\sqrt{\hbar\omega - E_g}$ [28,29,36]. It should be pointed out that the decreasing of Re χ, which is described by Eq. (B4), follows from the fact that ϵ_∞ is smaller than ϵ_b.

The effect of FK oscillations on feasible experimentally measurable optical functions is shown in Figs. 6(a) and 6(b). We have chosen the absorption coefficient α and the

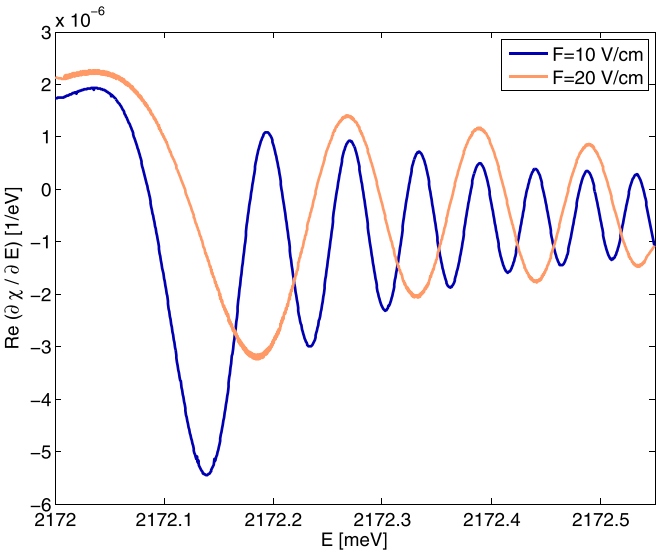

FIG. 4. The real part of the derivative Re $\partial\chi/\partial E$ displayed for the data in Fig. 1 for two values of the applied electric field.

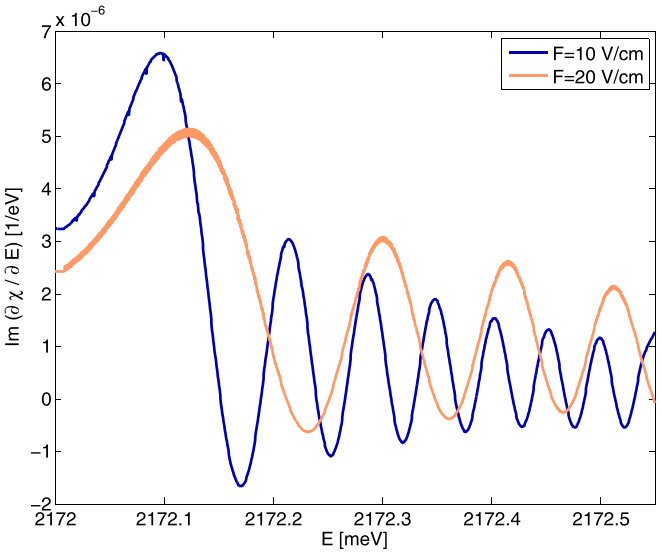

FIG. 5. The same as in Fig. 4 for the imaginary part of the susceptibility.

transmissivity T, for which we used the expressions

$$T = \frac{16|n|^2}{|(1+n)^2|^2}\, e^{-\alpha L} = \frac{16\left(n_1^2+n_2^2\right)}{\left[(1+n_1)^2-n_2^2\right]^2+4n_2^2(1+n_1)^2}\, e^{-\alpha L},$$
$$\alpha = 2\frac{\hbar\omega}{\hbar c}\mathrm{Im}\, n, \tag{29}$$

where n denotes the complex refraction coefficient $n = \sqrt{\epsilon_b+\chi} = n_1 + in_2$. When calculating the difference $\Delta T = T(F) - T(F=0)$, we use the expression for the zero-field susceptibility [see Eq. (A7)]

$$\chi(F=0) = \frac{\chi'}{1-1/2k}\left[2k\rho_0 + \sqrt{\pi}\left(1-2k^2\rho_0^2\right)w(ik\rho_0)\right]. \tag{30}$$

One can see that the oscillations in the absorption spectrum become smoother for higher electric field [Fig. 6(a)]. Moreover, the absorption increases with electric field, while the amplitude of oscillations remains almost unchanged. Similar effects are seen for the relative transmission coefficient [Fig. 6(b)], which is, in turn, lower for higher F. It can also be seen that the shape of the FK oscillations strongly depends on the damping parameter Γ, as shown in Figs. 7(a) and 7(b). The spectrum shows characteristic FK oscillations, and the positions of their minima and maxima are in perfect agreement with peaks for excitation energies predicted by Eq. (28). The amplitude of the oscillations is more pronounced for higher values of the damping parameter Γ which characterizes dissipative processes, e.g., the interaction between excitons (quasiparticles) and phonons. An external electric field accelerates particles, which leads to an increase in their energy and amplifies their coupling with the background. As a consequence, one can observe enlarged amplitudes of FK oscillations due to the increase in absorption for higher values of Γ. In Fig. 7(b), the full three-dimensional plot shows the dependence of FK

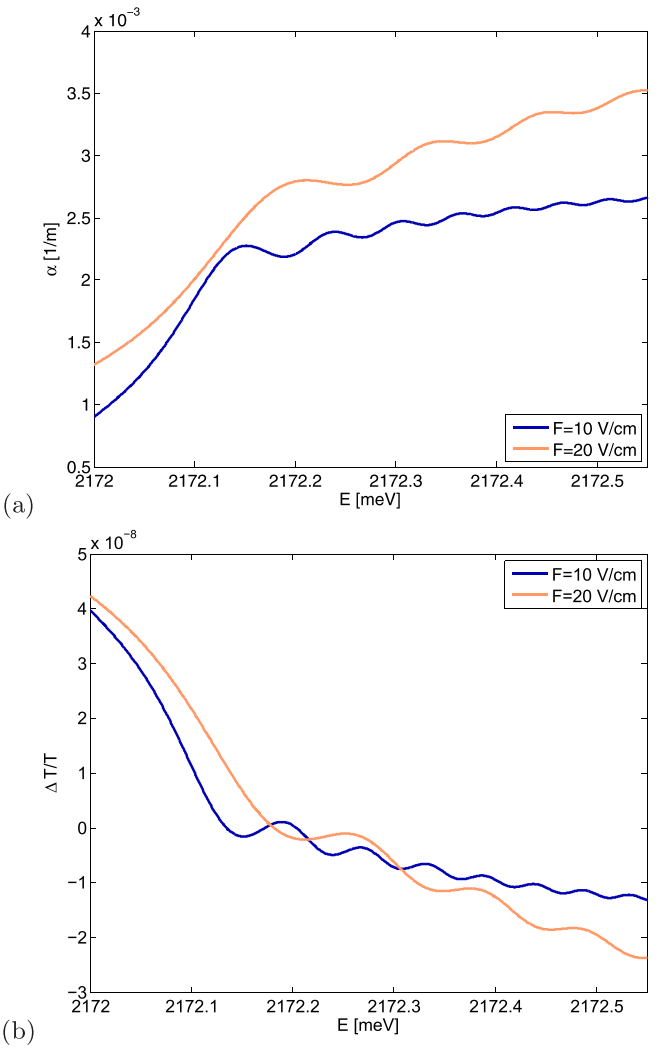

FIG. 6. (a) Absorption α and (b) relative transmission coefficient $\Delta T/T$ for two values of applied electric field F.

oscillations of the absorption spectrum on energy (above the gap) for a wide range of the damping parameter.

V. IMPACT OF HIGHER EXCITONIC STATES ON THE FRANZ-KELDYSH EFFECT

Above we have considered the Franz-Keldysh effect with one exciton state. Until now only the problem of the dependence of the multiplicity of excitonic states on the Franz-Keldysh effect for confined systems or for a system in an external magnetic field has been examined ([38] and references therein), and the general solution for bulk crystal is not available. Below we propose a method which allows us to study the effect of the two lowest exciton states. To achieve this goal we will consider the amplitude Y in the form

$$Y = Y_1 + Y_2, \tag{31}$$

where

$$Y_1 = N_1 Y_{01}\rho e^{i\phi} e^{-k\sqrt{\rho^2+\zeta^2}} = Y_{01}\psi_1,$$
$$Y_2 = N_2 Y_{02}\rho e^{i\phi}(3-k\sqrt{\rho^2+\zeta^2})e^{-(2k/3)\sqrt{\rho^2+\zeta^2}} = Y_{02}\psi_2 \tag{32}$$

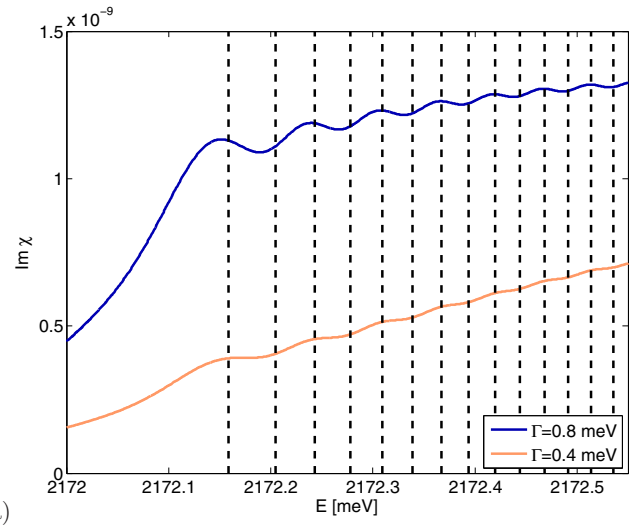

(a)

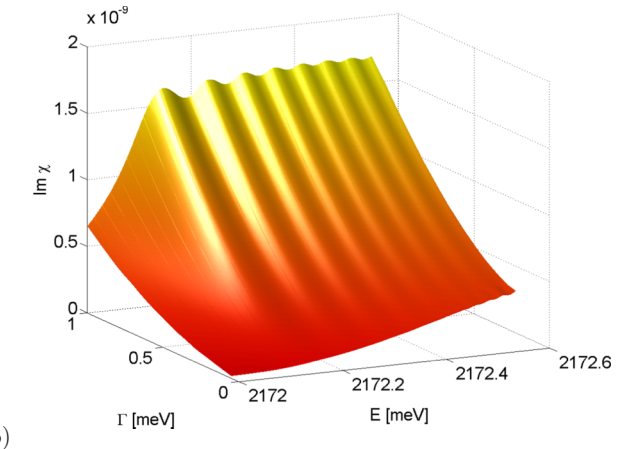

(b)

FIG. 7. (a) Imaginary part of the susceptibility for two values of Γ. Dashed lines mark the positions of extrema calculated from Eq. (28). (b) Imaginary part of the susceptibility for a range of values of Γ.

are orthogonal for k real (below the gap for $\Gamma = 0$) and N_1, N_2 represent the normalization factors of the resonance energies. In the above definitions we neglect the center-of-mass dependence.

The ansatz (31) contains two unknown parameters, Y_{01}, Y_{02}. They can be determined from the integral equation (17). One of the possible methods is to use the projection of those equations onto an orthonormal basis which yields equations for the parameters (Galerkin method). We choose the basis in the form

$$\varphi_1(\rho,\zeta,\phi) = \frac{1}{\sqrt{\pi}}\frac{\rho}{\rho_0^2}e^{i\phi}\exp\left(-\frac{\rho^2}{2\rho_0^2}\right)\delta(\zeta),$$
$$\varphi_2(\rho,\zeta,\phi) = \sqrt{\frac{2}{\pi}}\frac{\rho}{\rho_0^2}e^{i\phi}\left(1-\frac{\rho^2}{2\rho_0^2}\right)\exp\left(-\frac{\rho^2}{2\rho_0^2}\right)\delta(\zeta). \quad (33)$$

Using the common notation for the scalar product, we obtain the equations

$$\langle\varphi_1|Y\rangle = \langle\varphi_1|GM\rangle - \langle\varphi_1|GVY\rangle,$$
$$\langle\varphi_2|Y\rangle = \langle\varphi_2|GM\rangle - \langle\varphi_2|GVY\rangle, \quad (34)$$

where we neglect the constant factors. Inserting the expression for Y, we get from (34) the equations

$$a_{11}x_1 + a_{12}x_2 = b_1,$$
$$a_{21}x_1 + a_{22}x_2 = b_2, \quad (35)$$

where

$$x_1 = \frac{2}{\epsilon_0\mathcal{E}}M_0Y_{01}, \quad x_2 = \frac{2}{\epsilon_0\mathcal{E}}M_0Y_{02},$$
$$a_{11} = \langle\varphi_1|\psi_1\rangle - \langle\varphi_1|G\tilde{V}\psi_1\rangle, \quad (36)$$

and

$$a_{12} = \langle\varphi_1|\psi_2\rangle - \langle\varphi_1|G\tilde{V}\psi_2\rangle,$$
$$a_{21} = \langle\varphi_2|\psi_1\rangle - \langle\varphi_2|G\tilde{V}\psi_1\rangle,$$
$$a_{22} = \langle\varphi_2|\psi_2\rangle - \langle\varphi_2|G\tilde{V}\psi_2\rangle,$$
$$\tilde{V} = \frac{2}{\sqrt{\rho^2+\gamma\zeta^2}}, \quad \tilde{M} = \frac{M}{M_0},$$
$$b_1 = \frac{2\mu}{\hbar^2a^*}\frac{2M_0^2}{\epsilon_0}\langle\varphi_1|G\tilde{M}\rangle,$$
$$b_2 = \frac{2\mu}{\hbar^2a^*}\frac{2M_0^2}{\epsilon_0}\langle\varphi_2|G\tilde{M}\rangle. \quad (37)$$

The quantities x_1, x_2, b_1, b_2 are dimensionless; x_1, x_2 define the electrosusceptibility via the equation

$$\chi = x_1\langle M|\psi_1\rangle + x_2\langle M|\psi_2\rangle. \quad (38)$$

As done above, some information can be elicited by setting $V = 0$. After some simple algebra we obtain

$$x_1 = \frac{1}{\Delta}(b_1\langle\varphi_2|\psi_2\rangle - b_2\langle\varphi_1|\psi_2\rangle),$$
$$x_2 = \frac{1}{\Delta}(b_2\langle\varphi_1|\psi_1\rangle - b_1\langle\varphi_2|\psi_1\rangle),$$
$$\Delta = \langle\varphi_1|\psi_1\rangle\langle\varphi_2|\psi_2\rangle - \langle\varphi_1|\psi_2\rangle\langle\varphi_2|\psi_1\rangle. \quad (39)$$

Comparing the above outcomes with the aforementioned results for the one-exciton state we observe that an additional state (the same holds for more additional states) will influence only the shape and the amplitude of FK oscillations, while the periodicity will practically remain the same since it is involved in the Green's function. One can also say that the calculation, at least the analytical one, will be more intricate than in the case of the one-exciton state. As a consequence, the method described above is practically operational only for two-exciton states. However, it should also be stressed that the higher excitonic states are coupled with oscillator strengths decreasing as $1/n^3$, so their influence will be orders of magnitude smaller than the contribution of the two lowest states.

VI. RYDBERG EXCITONS IN A ONE-DIMENSIONAL MODEL

As we have discussed above, the simultaneous description of a multiplicity of excitonic states below the gap and the FK oscillations above the gap is, at the moment, not accessible. So considering the multiplicity of exciton states as the dominant feature of Rydberg excitons, we propose a simplified exciton model in which both phenomena can be described by analytical

formulas. To this end, we consider a system with reduced dimensionality, where an electron with the effective mass m_e and a hole with the effective mass m_{hz} move along the z axis. A constant electric field F is applied in the same direction. The optical properties of the system described in the previous sections will be described with the RDMA, starting from the constitutive equation (1), with the Hamiltonian (2), which now takes the form

$$H_{eh} = E_g - \frac{\hbar^2}{2m_e}\partial_{z_e}^2 - \frac{\hbar^2}{2m_{hz}}\partial_{z_h}^2 + eF(z_h - z_e) + V_{eh}(z_e - z_h) + V_e(z_e) + V_h(z_h). \tag{40}$$

In order to account for n excitonic states, we consider the system to be a set of independent oscillators which, in our formalism, will be related to the exciton amplitudes Y_n. The amplitudes will satisfy the equations

$$\left[E_g - \hbar\omega - i\Gamma_n - \frac{\hbar^2}{2\mu_z}\partial_z^2 + eFz + V_{ehn}(z)\right]Y_n(z) = M_n(z)E_0, \tag{41}$$

where E_0 is the amplitude of the electromagnetic wave propagating in the medium. The potentials V_{ehn} and the transition dipole matrix elements M_n will be chosen to reproduce the optical properties of Rydberg excitons. Equation (4) for the total polarization will be replaced by the relation

$$\mathbf{P}(\mathbf{R}) = 2\int d^3r\,\mathrm{Re}\left[\sum_n \mathbf{M}_n(\mathbf{r})Y_n(\mathbf{r},\mathbf{R})\right]. \tag{42}$$

Following the scheme described in Sec. III, we arrive at the equation

$$\left[k^2 - \partial_\zeta^2 + f\zeta\right]Y_n = \frac{2\mu_\parallel}{\hbar^2}a^{*2}\tilde{M}_n(\zeta)E_0 - \tilde{V}_{ehn}(\zeta)Y_n. \tag{43}$$

The Green's function of the above equation has the form [compare Eq. (19)]

$$G(\zeta,\zeta') = g^< g^>,$$
$$g^< = \frac{\pi}{f^{1/3}}\mathrm{Bi}\left[f^{\frac{1}{3}}\left(\zeta^< + \frac{k^2}{f}\right)\right] + i\,\mathrm{Ai}\left[f^{\frac{1}{3}}\left(\zeta^< + \frac{k^2}{f}\right)\right],$$
$$g^> = \mathrm{Ai}\left[f^{\frac{1}{3}}\left(\zeta^> + \frac{k^2}{f}\right)\right]. \tag{44}$$

When the external electric field is absent, the Green's function takes the form

$$G(\zeta,\zeta')_{F=0} = \frac{\exp(-k|\zeta - \zeta'|}{2k}. \tag{45}$$

Choosing $\tilde{M}_n$ and $\tilde{V}_{ehn}$ in the form

$$\tilde{M}_n = M_{0n}\delta(\zeta), \quad \tilde{V}_{ehn} = -2\sqrt{\varepsilon_{Tn}}\delta(\zeta), \tag{46}$$

we arrive at the following expression for the susceptibility:

$$\chi = \sum_n \frac{f_n G(0,0)}{1 - 2\sqrt{\varepsilon_{Tn}}G(0,0)}, \tag{47}$$

with oscillator strength, for which we can use the expressions derived in Ref. [10]. With respect to (45), for energies below the gap and for the field $F = 0$, we obtain

$$\chi = \sum_n \frac{f_n}{2(k - \sqrt{\varepsilon_{Tn}})}. \tag{48}$$

The poles in the susceptibility define the quantities ε_{Tn} which are related to the excitonic resonances energies $\hbar\omega_{Tn}$ by $\varepsilon_{Tn} = (E_g - \hbar\omega_{Tn})/R^*$. Note that formulas (47) and (48) are valid for both energies below and above the gap. They are obtained from a model different from that used in Ref. [10], which was applied for energies below the gap. Here excitonic states are described by appropriate harmonic oscillators. When considering the case of Cu_2O, the resonance energies are $\sqrt{\varepsilon_{Tn}}$, and the oscillator strengths are also well known, so the shapes of the susceptibility (for the energies below the gap) calculated with the help of both procedures are identical.

Considering the case of Cu_2O, we start with $n = 2$, and the oscillator strengths f_n will be chosen as

$$f_n = \epsilon_b\frac{\Delta_{LT}}{R^*}\frac{32}{3}\frac{n^2 - 1}{n^5}. \tag{49}$$

The absorption calculated by Eq. (48) gives an account of the qualitative behavior of the imaginary part of the susceptibility for energies below and above the gap. We obtain the resonances below the gap as well as the oscillations characteristic of the FK effect, but the magnitudes of the oscillations' amplitudes differ considerably in both energetic regions. Resonances below the gap amplify oscillations, while above the gap the lack of excitonic resonances causes a significant reduction. The Rydberg exciton states compose the background of the FK oscillations. When the electric field is applied, we use expression (47) with Green's function (44). As in the general considerations (see Sec. IV), we observe the FK oscillations.

The advantage of the method described in this section results from the fact that an arbitrary number of excitonic states can be taken into account; in such a case the optical functions display the impact of the increasing number of considered states. One can see that the period and phase of the oscillations do not depend on the excitonic state number n. This effect is illustrated in Fig. 8, which presents the impact on absorption of the number of excitonic states taken into account. As one might expect, the influence of higher excitonic states on FK oscillations is visible but not distinctive. This is due to the fact that oscillator strengths diminish as $1/n^3$, and since Δ_{LT}/R^* is of the order of 10^{-5}, the impact of additional excitons with higher n on spectra above the gap becomes subtle. This justifies our choice to take into account only one excitonic state (with the largest oscillator strength) as done in Sec. IV.

VII. DISCUSSION AND CONCLUSIONS

We have analyzed the optical properties of semiconductors with Rydberg excitons exposed to a static electric field. We have developed a simple mathematical procedure to calculate electro-optical functions of semiconductor crystal with symmetry where P-exciton transitions are dipole allowed. The presented method has been used to investigate electro-optical functions of Cu_2O crystal for the case of normal incidence and the static electric field applied in the same direction. For excitation energies larger than the fundamental gap we have obtained oscillations for optical functions which are identified

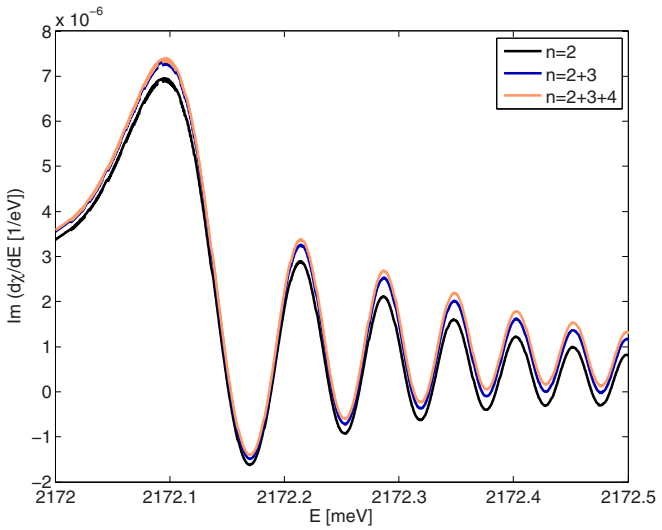

FIG. 8. The impact of the number of discrete excitonic states below the gap on the FK oscillations above the gap for $F = 10$ V/cm.

as Franz-Keldysh oscillations. Their periodicity with respect to the excitation energy, the amplitudes, and the dependence on the applied field strength was calculated and presented in the form of analytical expressions. The outcomes differ from the known results for the FK effect for S excitons. We have also examined the influence of the coherence of the carriers on dispersion $\mathrm{Re}\chi$.

The Franz-Keldysh effect provides an optoelectronic mechanism to create and control the electromodulations which might be an essential and flexible tool for constructing optical compatible output devices, e.g., a modulator or detectors with an off-chip laser. The copper oxide–based optoelectronic modulators employing the Franz-Keldysh effect might show great promise in meeting the strict energy requirements with controlled modification of the reflection/transmission modulation. It also seems that controlling the periodicity of FK oscillations may help determine the effective masses along propagation axes.

The experimental data for the FK effect in Cu_2O are not available yet, but we hope that our theoretical considerations might stimulate experiments of the electro-optical properties of this crystal for the above-gap regime. We conclude that the dynamical density-matrix approach is well suited to describe the macroscopic fields (static and dynamic) and the microscopic excitons in all limits of physical interest.

ACKNOWLEDGMENT

Support from the National Science Centre, Poland (project OPUS, CIREL 2017/25/B/ST3/00817), is greatly acknowledged.

APPENDIX A: THE DIPOLE TRANSITION MATRIX ELEMENT M_0

The polariton dispersion relation for the considered case has the form

$$\frac{c^2k_z^2}{\omega^2} = \epsilon(\omega,k_z,\Gamma) = \epsilon_b + \chi, \tag{A1}$$

with χ being the susceptibility. When the constant electric field is absent, the susceptibility has the form

$$\chi = \frac{2}{\epsilon_0}\frac{2\mu}{\hbar^2 a^*}\frac{M_0^2}{4\pi\rho_0}\left[2k\rho_0 + \sqrt{\pi}\left(1-2k^2\rho_0^2\right)w(ik\rho_0)\right] \times \frac{1}{1-1/2k}, \tag{A2}$$

where $w(z)$ is the complex error function [43],

$$w(z) = e^{-z^2}\left(1 + \frac{2i}{\sqrt{\pi}}\int_0^z e^{-t^2}dt\right) = e^{-z^2}[1-\mathrm{erf}(-iz)], \tag{A3}$$

and $\mathrm{erf}(z)$ is the common error function,

$$\mathrm{erf}(z) = \frac{2}{\sqrt{\pi}}\int_0^z e^{-t^2}dt. \tag{A4}$$

In our formalism the coherence effects are included in the dipole density function M (10), where M_0 is the integrated strength and is related to the coherence radius ρ_0. For the longitudinal mode $\epsilon = 0$ at $k_z = 0$ and $\Gamma = 0$, which gives the equation

$$\epsilon_b + \frac{2}{\epsilon_0}\frac{2\mu}{\hbar^2 a^*}\frac{M_0^2}{4\pi\rho_0}\left[2k_L\rho_0 + \sqrt{\pi}\left(1-2k_L^2\rho_0^2\right)w(ik_L\rho_0)\right] \times \frac{1}{1-1/2k_L} = 0, \tag{A5}$$

where we denoted

$$k_L = k(\omega_L) = \left(\frac{E_g - \hbar\omega_L}{R^*}\right)^{1/2}. \tag{A6}$$

Introducing the quantity χ' [Eq. (22)], we express the total dielectric function for the case without applied field as

$$\epsilon(\omega) = \epsilon_b + \frac{\chi'}{1-1/2k}\left[2k\rho_0 + \sqrt{\pi}\left(1-2k^2\rho_0^2\right)w(ik\rho_0)\right] \tag{A7}$$

and transform Eq. (A5) into the form

$$\epsilon_b + \chi'\left[2k_L\rho_0 + \sqrt{\pi}\left(1-2k_L^2\rho_0^2\right)w(ik_L\rho_0)\right]\frac{1}{1-1/2k_L} = 0. \tag{A8}$$

Since, for the P exciton, $k_L \approx 1/2$ and

$$\frac{1}{1-1/2k_L} \approx -\frac{R^*}{2\Delta_{LT}}, \tag{A9}$$

we obtain from (A8)

$$\chi' = \frac{2\epsilon_b\Delta_{LT}}{R^*}\left[2k_L\rho_0 + \sqrt{\pi}\left(1-2k_L^2\rho_0^2\right)w(ik_L\rho_0)\right]^{-1}. \tag{A10}$$

The above equation determines the relation between the quantity χ' (and thus the matrix element M_0) and the coherence radius ρ_0. For a given value of ρ_0 we determine the quantity χ', which is then used in the expressions for the susceptibility. As stated in Ref. [36], the relation (A5) determines the value of M_0^2/ρ_0; to determine separately the matrix element M_0 and the coherence radius ρ_0, we need some more information about the behavior of the susceptibility at energies far above the excitonic resonances.

APPENDIX B: ASYMPTOTIC BEHAVIOR

As we have shown above, the optical properties of the excitation energy exceeding the fundamental gap are mainly determined by the behavior of the numerator in Eq. (21). For the Cu_2O data the expression $\rho_0^2 x^2$ is small in the relevant interval of x. Therefore we can expand $\exp(-\rho_0^2 x^2)$ and perform the integration involving Airy functions [49]. In the lowest order and for $\Gamma \to 0$ we obtain

$$\begin{aligned}\mathrm{Re}\,\chi &= \frac{2\pi\chi'\rho_0^3}{Q}\left(\frac{\hbar\Theta}{R^*}\right)^{3/2}\frac{1}{6}\left[4\mathcal{E}\mathrm{Ai}'\mathrm{Bi}' + 4\mathcal{E}^2\mathrm{AiBi} - \mathrm{Ai}'\mathrm{Bi} - \mathrm{AiBi}'\right]\\ &= \frac{2\pi\chi'\rho_0^3}{Q}\left\{\frac{2}{3}\left(\frac{\hbar\Theta}{R^*}\right)^{1/2}\left(\frac{\hbar\omega - E_g}{R^*}\right)\mathrm{Ai}'\left(-\frac{\hbar\omega - E_g}{\hbar\Theta}\right)\mathrm{Bi}'\left(-\frac{\hbar\omega - E_g}{\hbar\Theta}\right) + \frac{2}{3}\left(\frac{R^*}{\hbar\Theta}\right)^{1/2}\left(\frac{\hbar\omega - E_g}{R^*}\right)^2\right.\\ &\quad\times\mathrm{Ai}\left(-\frac{\hbar\omega - E_g}{\hbar\Theta}\right)\mathrm{Bi}\left(-\frac{\hbar\omega - E_g}{\hbar\Theta}\right) - \frac{1}{6}\left(\frac{\hbar\Theta}{R^*}\right)^{3/2}\mathrm{Ai}'\left(-\frac{\hbar\omega - E_g}{\hbar\Theta}\right)\mathrm{Bi}\left(-\frac{\hbar\omega - E_g}{\hbar\Theta}\right) - \frac{1}{6}\left(\frac{\hbar\Theta}{R^*}\right)^{3/2}\\ &\quad\left.\times\mathrm{Ai}\left(-\frac{\hbar\omega - E_g}{\hbar\Theta}\right)\mathrm{Bi}'\left(-\frac{\hbar\omega - E_g}{\hbar\Theta}\right)\right\}, \qquad \text{(B1)}\\ \mathrm{Im}\,\chi &= \frac{2\pi\chi'\rho_0^3}{Q}\left\{-\frac{1}{3}\left(\frac{\hbar\Theta}{R^*}\right)^{3/2}\mathrm{Ai}'\left(-\frac{\hbar\omega - E_g}{\hbar\Theta}\right)\mathrm{Ai}\left(-\frac{\hbar\omega - E_g}{\hbar\Theta}\right) + \frac{2}{3}\left(\frac{\hbar\Theta}{R^*}\right)^{1/2}\left(\frac{\hbar\omega - E_g}{R^*}\right)\mathrm{Ai}'^2\left(-\frac{\hbar\omega - E_g}{\hbar\Theta}\right)\right.\\ &\quad\left.+\frac{2}{3}\left(\frac{R^*}{\hbar\Theta}\right)^{1/2}\left(\frac{\hbar\omega - E_g}{R^*}\right)^2\mathrm{Ai}^2\left(-\frac{\hbar\omega - E_g}{\hbar\Theta}\right)\right\}, \qquad \text{(B2)}\end{aligned}$$

with χ' defined in Eq. (22).

Note that the above expressions differ from the expressions for S excitons (allowed interband transitions, for example, GaAs) [28,29,36],

$$\mathrm{Im}\,\chi \propto \left\{\frac{\hbar\omega - E_g}{\hbar\Theta}\mathrm{Ai}^2\left(-\frac{\hbar\omega - E_g}{\hbar\Theta}\right) + \left[\mathrm{Ai}'\left(-\frac{\hbar\omega - E_g}{\hbar\Theta}\right)\right]^2\right\}. \qquad \text{(B3)}$$

Having in mind the properties of Cu_2O, we observe that the value of the electro-optical energy $\hbar\Theta$ is small compared to the Rydberg energy. Therefore the arguments of the Airy functions in expressions (B1) and (B2) quickly reach the values which justify the use of their asymptotic expansions, giving in the lowest order with respect to ζ the formulas for the real and imaginary parts of the susceptibility,

$$\mathrm{Re}\,\chi \to -\frac{\chi'\rho_0^3}{3Q}\left(\frac{\hbar\Theta}{R^*}\right)^{3/2}\sin 2\zeta, \quad \mathrm{Im}\,\chi \to \frac{\chi'\rho_0^3}{Q}\left(\frac{\hbar\Theta}{R^*}\right)^{3/2}\cos 2\zeta + \frac{4\chi'\rho_0^3}{3Q}\left(\frac{\hbar\omega - E_g}{R^*}\right)^{3/2}, \quad \zeta = \frac{2}{3}\left(\frac{\hbar\omega - E_g}{\hbar\Theta}\right)^{3/2}. \qquad \text{(B4)}$$

The above expressions allow us to get the periodicity of the FK oscillations; the peaks will appear at energies given in Eq. (28).

[1] D. Fröhlich, A. Kulik, B. Uebbing, A. Mysyrowicz, V. Langer, H. Stolz, and W. von der Osten, Coherent Propagation and Quantum Beats of Quadrupole Polaritons in Cu_2O, Phys. Rev. Lett. **67**, 2343 (1991).

[2] S. Nikitine, Experimental investigations of exciton spectra in ionic crystals, Philos. Mag. **4**, 1 (1959).

[3] D. Fröhlich and R. Kenklies, Polarization dependence of two-photon magnetoabsorption of the 1s exciton in Cu_2O, Phys. Status Solidi B **111**, 247 (1982).

[4] J. Ghijsen, L. H. Tjeng, J. van Elp, H. Eskes, J. Westerink, G. A. Sawatzky, and M. T. Czyzyk, Electronic structure of Cu_2O and CuO, Phys. Rev. B **38**, 11322 (1988).

[5] A. Jolk, M. Jörger, and C. Klingshirn, Exciton lifetime, Auger recombination, and exciton transport by calibrated differential absorption spectroscopy in Cu_2O, Phys. Rev. B. **65**, 245209 (2002).

[6] M. Jörger, T. Fleck, C. Klingshirn, and R. von Baltz, Midinfrared properties of cuprous oxide: High-order lattice vibrations and intraexcitonic transitions of the 1s paraexciton, Phys. Rev. B **71**, 235210 (2005).

[7] H. Stolz, R. Schwartz, F. Kieseling, S. Som, M. Kaupsch, S. Sobkowiak, D. Semkat, N. Naka, T. Koch, and H. Fehske, Condensation of excitons in Cu_2O at ultracold temperatures: Experiment and theory, New J. Phys. **14**, 105007 (2012).

[8] T. Kazimierczuk, D. Fröhlich, S. Scheel, H. Stolz, and M. Bayer, Giant Rydberg excitons in the copper oxide Cu_2O, Nature (London) **514**, 343 (2014).

[9] J. Thewes, J. Heckötter, T. Kazimierczuk, M. Aßmann, D. Fröhlich, M. Bayer, M. A. Semina, and M. M. Glazov, Observation of High Angular Momentum Excitons in Cuprous Oxide, Phys. Rev. Lett. **115**, 027402 (2015).

[10] S. Zielińska-Raczyńska, G. Czajkowski, and D. Ziemkiewicz, Optical properties of Rydberg excitons and polaritons, Phys. Rev. B **93**, 075206 (2016).

[11] F. Schöne, S.-O. Krüger, P. Grünwald, H. Stolz, M. Aßmann, J. Heckötter, J. Thewes, D. Fröhlich, and M. Bayer, Deviations of

the exciton level spectrum in Cu_2O from the hydrogen series, Phys. Rev. B **93**, 075203 (2016).
[12] F. Schweiner, J. Main, and G. Wunner, Linewidths in excitonic absorption spectra of cuprous oxide, Phys. Rev. B **93**, 085203 (2016).
[13] P. Grünwald, M. Aßmann, J. Heckötter, D. Fröhlich, M. Bayer, H. Stolz, and S. Scheel, Signatures of Quantum Coherences in Rydberg Excitons, Phys. Rev. Lett. **117**, 133003 (2016).
[14] J. Heckötter, M. Freitag, D. Fröhlich, M. Aßmann, M. Bayer, M. A. Semina, and M. M. Glazov, Scaling laws of Rydberg excitons, Phys. Rev. B **96**, 125142 (2017).
[15] F. Schweiner, J. Main, G. Wunner, and Ch. Uihlein, Even exciton series in Cu_2O, Phys. Rev. B **95**, 195201 (2017).
[16] F. Schweiner, J. Ertl, J. Main, G. Wunner, and Ch. Uihlein, Exciton-polaritons in cuprous oxide: Theory and comparison with experiment, Phys. Rev. B **96**, 245202 (2017).
[17] V. Walther, R. Johne, and T. Pohl, Giant optical nonlinearities from Rydberg excitons in semiconductor microcavities, Nat. Commun. **9**, 1309 (2018).
[18] S. Zielińska-Raczyńska, D. Ziemkiewicz, and G. Czajkowski, Electro-optical properties of Rydberg excitons, Phys. Rev. B **94**, 045205 (2016).
[19] F. Schweiner, J. Main, G. Wunner, M. Freitag, J. Heckötter, Ch. Uihlein, M. Aßmann, D. Fröhlich, and M. Bayer, Magnetoexcitons in cuprous oxide, Phys. Rev. B **95**, 035202 (2017).
[20] S. Zielińska-Raczyńska, D. Ziemkiewicz, and G. Czajkowski, Magneto-optical properties of Rydberg excitons: Center-of-mass quantization approach, Phys. Rev. B **95**, 075204 (2017).
[21] M. Aßmann, J. Thewes, and M. Bayer, Quantum chaos and breaking of all antiunitary symmetries in Rydberg excitons, Nat. Mater. **15**, 741 (2016).
[22] F. Schweiner, P. Rommel, J. Main, and G. Wunner, Exciton-phonon interaction breaking all antiunitary symmetries in external magnetic fields, Phys. Rev. B **96**, 035207 (2017).
[23] F. Schweiner, J. Main, and G. Wunner, Magnetoexcitons Break Antiunitary Symmetries, Phys. Rev. Lett. **118**, 046401 (2017).
[24] T. Kitamura, M. Takahata, and N. Naka, Quantum number dependence of the photoluminescence broadening of excitonic Rydberg states in cuprous oxide, J. Lumin. **192**, 808 (2017).
[25] J. Heckötter, M. Freitag, D. Fröhlich, M. Aßmann, M. Bayer, P. Grünwald, F. Schöne, D. Semkat, H. Stolz, and S. Scheel, Rydberg excitons in the presence of an ultralow-density electron-hole plasma, arXiv:1709.00891.
[26] W. Franz, Einfluß eines elektrischen Feldes auf eine optische Absorptionskante, Z. Naturforsch. **13a**, 484 (1958).
[27] L. V. Keldysh, Behavior of non-metallic crystals in strong electric fields, Zh. Eksp. Teor. Fiz. **33**, 994 (1957) [Sov. Phys. JETP **6**, 763 (1958)].
[28] K. Tharmalingam, Optical Absorption in the Presence of a Uniform Field, Phys. Rev. **130**, 2204 (1963).
[29] K. S. Viswanathan and J. Callaway, Dielectric Constant of a Semiconductor in an External Electric Field, Phys. Rev. **143**, 564 (1966).
[30] H. I. Ralph, On the theory of Franz-Keldysh effect, J. Phys. C **1**, 378 (1968).
[31] D. F. Blossey, Wannier exciton in an electric field. I. Optical absorption by bound and continuum states, Phys. Rev. B **2**, 3976 (1970).
[32] D. F. Blossey, Wannier exciton in an electric field. II. Electroabsorption in direct-band-gap solids, Phys. Rev. B **3**, 1382 (1971).
[33] B. Schlichterle, G. Weiser, M. Klenk, F. Mollot, and Ch. Starck, Effective masses in $In_{1-x}Ga_xAs$ superlattices derived from Franz-Keldysh oscillations, Phys. Rev. B **52**, 9003 (1995).
[34] M. Nakayama, T. Nakanishi, K. Okajima, M. Ando, and H. Nishimura, Miniband structures and effective masses of GaAs/AlAs superlattices with ultra-thin layers, Solid State Commun. **102**, 803 (1997).
[35] H. Shen and M. Dutta, Franz-Keldysh oscillations in modulation spectroscopy, J. Appl. Phys. **78**, 2151 (1995).
[36] G. Czajkowski, M. Dressler, and F. Bassani, Electro-optical properties of semiconductor superlattices in the regime of Franz-Keldysh oscillations, Phys. Rev. B **55**, 5243 (1997).
[37] A. Jaeger and G. Weiser, Excitonic electroabsorption spectra and Franz-Keldysh effect of $In_{0.53}Ga_{0.47}As/InP$ studied by small modulation of static fields, Phys. Rev. B **58**, 10674 (1998).
[38] G. Czajkowski, F. Bassani, and L. Silvestri, Excitonic optical properties of nanostructures: Real density matrix approach, Riv. Nuovo Cimento **26**, 1 (2003).
[39] J. R. Madureira, M. Z. Maialle, and M. H. Degani, Franz-Keldysh effect in semiconductor T-wire in applied magnetic field, Braz. J. Phys. **34**, 663 (2004).
[40] R. K. Schaevitz, D. S. Ly-Gagnon, J. E. Roth, E. H. Edwards, and D. A. B. Miller, Indirect absorption in germanium quantum wells, AIP Adv. **1**, 032164 (2011).
[41] S. J. Lee, Ch. W. Sohn, H.-J. Jo, I. S. Han, J. S. Kim, S. K. Noh, H. Choi, and J.-Y. Leem, Temperature dependence of the photovoltage from Franz-Keldysh oscillations in a GaAs p^+-i-n^+ structure, J. Korean Phys. Soc. **67**, 916 (2015).
[42] N. Botka, Micro photoreflectance semiconductor wafer analyzer, US Patent No. 5365334 A, 1994; M. L. Gray, H. F. Hess, M. S. Hybertsen, and L. J.-P. Ketelsen, Photoreflectance spectral analysis of semiconductor laser structures, US Patent No. 6195166 B1, 1999; T. Hideo and Y. Yoshitsugu, Optical measuring method for semiconductor multiple layer structures and apparatus therefor, US Patent No. 7038768 B2, 2003.
[43] *Handbook of Mathematical Functions*, edited by M. Abramowitz and I. Stegun (Dover, New York, 1965).
[44] E. T. Whittaker and G. N. Watson, *A Course of Modern Analysis*, 4th ed., Cambridge Mathematical Library (Cambridge University Press, Cambridge, 1996).
[45] I. S. Gradshteyn and I. M. Ryzhik, *Table of Integrals, Series, and Products*, 7th ed., edited by A. Jeffrey and D. Zwillinger (Academic, Amsterdam, 2007).
[46] N. Naka, I. Akimoto, M. Shirai, and K.-i. Kan'no, Time-resolved cyclotron resonance in cuprous oxide, Phys. Rev. B **85**, 035209 (2012).
[47] H. Stolz, F. Schöne, and D. Semkat, Interaction of Rydberg excitons in cuprous oxide with phonons and photons: Optical linewidth and polariton effect, New J. Phys. **20**, 023019 (2018).
[48] S. Zielińska-Raczyńska, G. Czajkowski, and D. Ziemkiewicz, Electro-optical properties of Cu_2O in the regime of Franz-Keldysh oscillations, arXiv:1712.02681.
[49] O. Vallée and M. Soares, *Airy Functions and Applications to Physics* (Imperial College Press, London, 2004).